Abdelaziz, A. E.; Hendy, Y. H. M.; Shokry, A.; Saad, S. M.; Kamal, F. Y.; Edris, K. A.

An astrometric and photometric study of the intermediate-age
open cluster NGC 2158 and its eclipsing binary [NBN2015]78

AN ASTROMETRIC AND PHOTOMETRIC STUDY OF THE INTERMEDIATE-AGE OPEN CLUSTER NGC 2158 AND ITS ECLIPSING BINARY [NBN2015]78

A. E. Abdelaziz[1], Y. H. M. Hendy[1], A. Shokry[1], S. M. Saad[1,2], F. Y. Kamal[3], and K. A. Edris[3]

ABSTRACT

We present a photometric and astrometric analysis of the NGC 2158 cluster using Gaia DR2 and 2MASS data. The cluster age, color excess, intrinsic distance modulus and distance are calculated to be $t = 2.240 \pm 0.260 \, \text{Gyr}$, $E(B - V) = 0.420 \pm 0.050 \, \text{mag}$, $(m - M)_\odot = 12.540 \pm 0.130 \, \text{mag}$ and $d_\odot = 3224 \pm 200 \, \text{pc}$ respectively. The photometric analysis and light curve modelling of the proposed eclipsing binary member [NBN2015]78 is performed using the latest version of the Wilson-Devinney (W-D) code. The solutions show that the system is an over-contact binary with a secondary component filling its Roche lobe, with a mass ratio $q = 0.262$. The primary and the secondary components of the system consist of two late spectral types K1 and K2 respectively. The membership of [NBN2015]78 is discussed using two independent methods, and we find that [NBN2015]78 is an interloper and not a member of NGC 2158.

RESUMEN

Presentamos un análisis fotométrico y astrométrico del cúmulo NGC 2158 con datos de Gaia DR2 y 2MASS. Calculamos la edad del cúmulo, el exceso de color, el módulo intrínseco de distancia y la distancia como $t = 2.240 \pm 0.260 \, \text{Giga-años}$, $E(B - V) = 0.420 \pm 0.050 \, \text{mag}$, $(m - M)_\odot = 12.540 \pm 0.130 \, \text{mag}$ y $d_\odot = 3224 \pm 200 \, \text{pc}$, respectivamente. Mediante la última versión del código Wilson-Devinney modelamos la curva de luz de la binaria eclipsante [NBN2015]78 propuesta como miembro del cúmulo. Las soluciones muestran que el sistema es una binaria en sobre-contacto, cuya secundaria llena el lóbulo de Roche; el cociente de masas es $q = 0.262$. Las dos componentes del sistema son de tipo espectral tardío, K1 y K2. Discutimos la pertenencia de [NBN2015]78 al cúmulo mediante dos métodos independientes, y encontramos que no pertenece a él.

Key Words: astrometry — binaries: eclipsing — open clusters and associations: individual: NGC 2158 — stars: individual: [NBN2015]78 — techniques: photometric

1. INTRODUCTION

Photometric studies of open clusters in the optical and infrared are fundamental tools for determining their structural parameters. These parameters play an important role towards understanding galactic structure and evolution. NGC 2158 [Melotte 40] is a rich northern open cluster of in-

[1]Astronomy Department, National Research Institute of Astronomy and Geophysics (NRIAG), Helwan, Cairo, Egypt.

[2]Kottamia Center of Scientificc Excellence for Astronomy and Space Sciences (KCScE), STDF No. 5217.

[3]Department of Astronomy and Meteorology, Faculty of Science, Al-Azhar University, Cairo, Egypt.

termediate age, located in the constellation Gemini (Carraro et al. 2002). It has a diameter of about $5'$ (Lynga et al. 1987). Anderson et al. (2013) estimated a core radius $R_{cor} = 1'.7$ and a limiting radius $R_{lim} = 18'.60$. Bedin et al. (2010) estimated log(age)=9.301, $E(B-V) = 0.420 \, \text{mag}$, $(m-M)_\odot = 12.980 \, \text{mag}$. Kharchenko et al. (2013) determined log (age) = 9.330, $E(B - V) = 0.333 \, \text{mag}$ and a heliocentric distance of $d_\odot = 4770 \, \text{pc}$. NGC 2158 is centered at (RA=06:07:25.00, DE=+24:05:48.00) and the eclipsing binary [NBN2015]78 is located at (RA=06:07:38.02, DE=+24:07:24.94), Figure 1 dis-
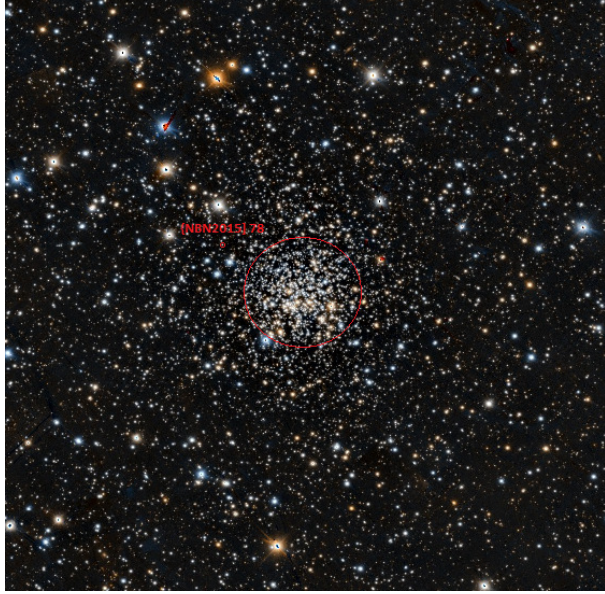
Fig. 1. Color image of the open cluster NGC 2158 from the Pan-STARRS survey (Panoramic Survey Telescope and Rapid Response System). The size of the field of view is $21' \times 21'$. The large red circle marks the region of the open cluster NGC 2158, while the small red circle gives the position of the eclipsing binary [NBN2015]78. The color figure can be viewed online.

plays the color image of the cluster using ALADIN (Bonnarel et al. 2000).

Studying eclipsing binary systems in the field and clusters gives valuable information about the physical and absolute parameters of the stars, such as masses and radii. Eclipsing binaries of the W UMa type are very important objects to study the evolutionary state of close binary stars and to characterize their formation. When they are members of a stellar cluster, the distance, age and metallicity of these stars are known independently, which makes them an ideal test for theories of binary structure and evolution. [NBN2015]78 is a poorly studied early-type eclipsing binary star which is located in the field of the open cluster NGC 2158. The designation comes from Nardiello et al. (2015), as it is the number 78 in their catalogue. It is also known as NGC 2158 MSS V60, NGC 2168 HIZ V6, and 2MASS J06073800 +2407249. It is a short period (0.341325 days) eclipsing binary system (Nardiello et al. 2015).

The main aim of this work is to present the photometric and astrometric parameters for the open cluster NGC 2158 and to perform a light curve analysis and modelling of the eclipsing binary [NBN2015]78. This paper is organized as follows: the photometric

and astrometric study of the open cluster NGC 2158 is presented in § 2. The photometric study of the eclipsing binary [NBN2015]78 is presented in § 3. Finally, discussions and conclusions are summarized in § 4.

2. PHOTOMETRIC AND ASTROMETRIC STUDY OF THE OPEN CLUSTER NGC 2158

2.1. Data and Analysis

In the present work, we use both the GAIA DR2 and 2MASS databases. Astrometric, photometric and spectroscopic measurements of the entire sky have been obtained by the ESA mission Gaia (Gaia Collaboration et al. 2016). The latest version of the Gaia data (Gaia DR2) contains over 1.3 billion sources in three photometric bands (G, G_{BP}, G_{RP}), in addition to their proper motion and parallax (Gaia Collaboration et al. 2018, Lindegren et al. 2018). The limiting G-band magnitude of Gaia DR2 data is 21 mag. At the bright end ($G < 14$ mag), the uncertainties reach 0.02 mas in parallax and 0.05 mas/yr in proper motions, while for sources near $G \sim 21$ mag the uncertainties reach 2 mas and 5 mas/yr respectively. The 2MASS survey is the catalog of choice for astronomical studies near the Galactic plane (Skrutskie et al. 2006). The limiting magnitudes of 2MASS data $J(1.25~\mu m)$, $H(1.65~\mu m)$ and $K(2.17\mu m)$ are 15.8, 15.1 and 14.3 mag, respectively.

We extracted the data around NGC 2158 inserting the coordinates of the cluster NGC 2158 as RA=06h 07m 25s.00, DEC=+24° 05′ 48″00, ℓ=186°634 and b=+1°781 (Dias et al. 2002) in the Virtual Observatory tool TOPCAT (Taylor 2005), within a radius of 30′. Cross-matching the Gaia DR2 and 2MASS data we obtain a matched number of stars of 17977.

To obtain the best astrometric precision of the proper motions, we used the sources brighter than $G = 18$ mag, which correspond to typical astrometric uncertainties smaller than 0.3 mas/yr in proper motion (Cantat-Gaudin et al. 2018, Lindegren et al. 2018). Using the Vector Point Diagram (VPD) of the proper motions in RA and DEC, we select the overdensity in the cluster region, obtaining 2103 stars (red region on the left panel, Figure 2). To obtain the candidate cluster members, we removed stars from the selected cluster region (red region) if their proper motions in RA and DEC were inconsistent with a median proper motion by more than three median absolute deviations (MAD). The color magnitude diagram (CMD) in the right panel of Figure 2 shows that the candidate members (red dots) fall on
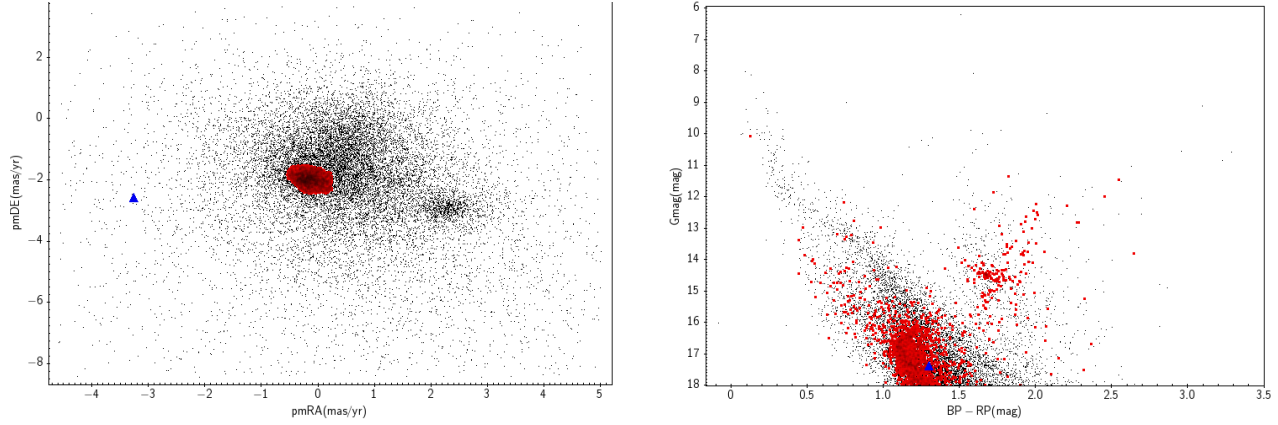
Fig. 2. The left panel shows the Vector Point Diagram (VPD), and the right panel shows the Color Magnitude Diagram (CMD) of the open cluster NGC 2158. The selected red region from the VPD marks the candidate member stars. The blue triangle and the black dots represent the eclipsing binary [NBN2015]78 and the field stars respectively. The red dots on the CMD represent candidate members. The color figure can be viewed online.
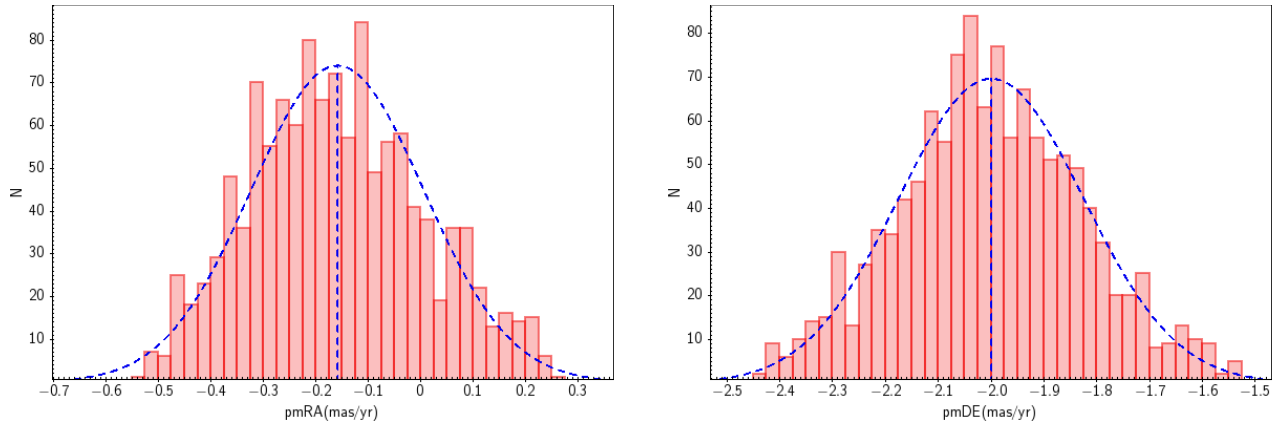

Fig. 3. The histograms of the proper motion in RA (mas/yr) and DEC (mas/yr), and the Gaussian fits are shown as blue dashed lines. The color figure can be viewed online.

a well-defined main sequence. The selected cluster region of the candidate members has a nearly ellipsoidal shape. The equivalent radius $R_e = \sqrt{a^2 + b^2}$ (with a and b the semi-major and semi-minor axes of the ellipse, respectively) of the selected cluster region is 0.7 mas/yr. This value is well within the range of the best-precision Gaia proper motions of 2 mas/yr (Ferreira et al. 2019).

Our membership criterion depends on the chosen overdensity region to define the members of the cluster from the VPD, which obviously is a compromise between losing cluster members and including field stars (see Bisht et al. 2019). To minimize the field contamination, we used the Blob subset from TOPCAT for selecting the cluster region in the VPD. Stars are considered members if they lie inside the

overdensity cluster region in VPD and have proper motions in RA and DEC within ±3 MAD from the mean proper motion; they must also have a clear main sequence in the CMD (Figure 2). These stars must be inside the limiting radius and they should have the same direction of proper motion vectors (Figure 4). The cluster members must have the same angular speed in the space.

To determine the mean proper motion of the cluster, we constructed the histograms and made a Gaussian fitting of the proper motions in both directions RA and DEC, see Figure 3. We found that the mean proper motion of NGC 2158 is pmRA $= -0.159 \pm 0.165$ mas/yr and pmDEC $= -2.000 \pm 0.175$ mas/yr. These values are in good

TABLE 1

ESTIMATION OF THE pm*RA* AND THE pm*DEC* VALUES OF THE OPEN CLUSTER NGC 2158

Parameter	Values	References
pmRA (mas/yr)	-0.159 ± 0.165	Present study
	-0.177 ± 0.185	Cantat-Gaudin et al. (2018)
	$+0.002 \pm 0.089$	Loktin and Popova (2017)
	-0.290	Kharchenko et al. (2013)
	$+1.430$	Wu et al. (2009)
	-1.220 ± 0.190	Dias et al. (2002)
pmDEC (mas/yr)	-2.000 ± 0.175	Present study
	-2.002 ± 0.173	Cantat-Gaudin et al. (2018)
	-0.849 ± 0.089	Loktin and Popova (2017)
	-2.480	Kharchenko et al. (2013)
	-3.280	Wu et al. (2009)
	-3.300 ± 0.010	Dias et al. (2002)

agreement with the values obtained by Cantat-Gaudin et al. (2018), see Table 1.

The measured proper motions of the eclipsing binary [NBN2015]78 in Gaia DR2 are pmRA = -3.252 ± 0.673 mas/yr and pmDEC = -2.63 ± 0.596 mas/yr with relative uncertainties smaller than 20%. The position of the eclipsing binary [NBN2015]78 in VPD is found to be very far away from the cluster region, close to the main sequence of the CMD (Figure 2). It is clearly seen that the direction of the proper motion vector of [NBN2015]78 in Figure 4 is different from the direction of the cluster members. Therefore, in spite of its position in the color magnitude diagrams in the optical and IR (2MASS, Figure 7) this eclipsing binary does not seem to be a member of the cluster.

2.2. Cluster Center and Radius

To determine the cluster center we count the stars in right ascension (RA) and declination (DEC). The center of the open cluster NGC 2158 is calculated at the point where the maximum stellar density of the cluster's area is reached, using a Gaussian fitting. The center of the cluster NGC 2158 is found to be at $RA = 91\overset{\circ}{.}866 \pm 0\overset{\circ}{.}077$ and $DEC = 24\overset{\circ}{.}109 \pm 0\overset{\circ}{.}070$, and the corresponding Galactic coordinates are $\ell = 186\overset{\circ}{.}629$ and $b = +1\overset{\circ}{.}796$ (Figure 5). We find that that the difference between our estimation of the centre of the cluster in RA and DEC and that of Cantat-Gaudin et al. (2018) is $14\overset{''}{.}4$ and $0\overset{'}{.}60$, respectively. The difference with the values from Anderson et al. (2013); Wu et al. (2009); Dias et al. (2002) is $43\overset{''}{.}2$ and $0\overset{'}{.}72$, respectively (Table 2).
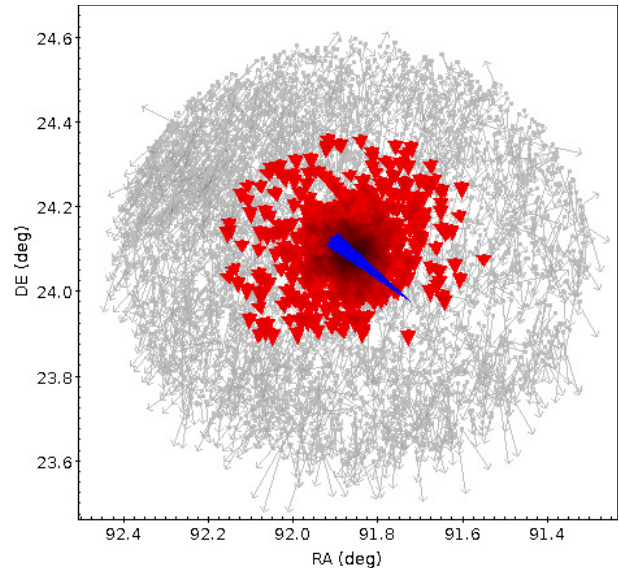

Fig. 4. Projection on the sky of the proper motion vectors. The red vectors (red triangles) represent the cluster members, the blue vector (blue triangle) represents the eclipsing binary [NBN2015]78 and the gray vectors (gray arrows) represent the field stars. The color figure can be viewed online.

To calculate the core and limiting radii, we measure the radial density profile (RDP) of the open cluster NGC 2158, extracting the brightest stars $G \leq 18$ mag within a square region of side 2 mas/yr around the center of the overdensity in the VPD, see Figure 2. We then divide the square area around the cluster into concentric rings. The stars are counted
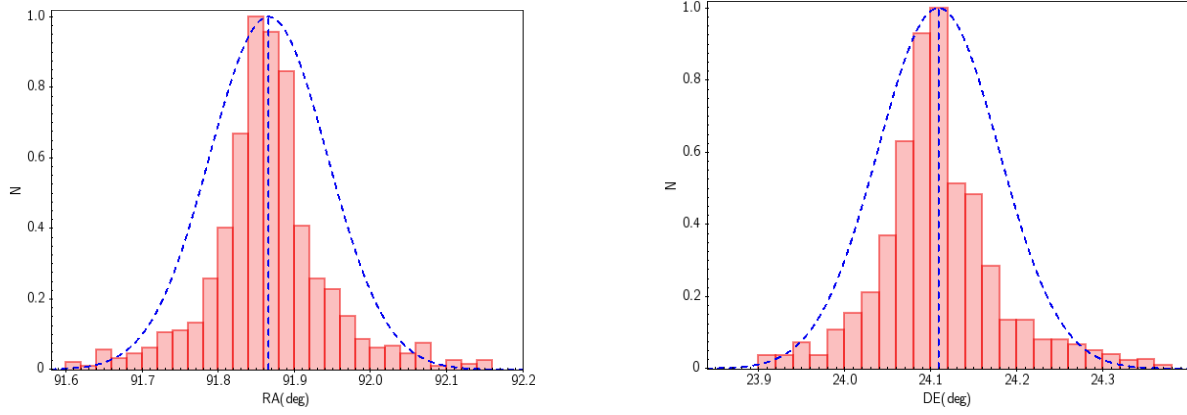
Fig. 5. Inferring the center of NGC 2158 in *RA* (left panel) and *DEC* (right panel). The blue lines are Gaussian fits. The color figure can be viewed online.

TABLE 2

ESTIMATIONS OF THE CENTER OF THE OPEN CLUSTER NGC 2158

Parameter	Values	References
RA (deg)	91.866±0.077	Present study
RA (hh:mm:ss)	06:07:27.84	Present study
	06:07:26.88	Cantat-Gaudin et al. (2018)
	06:07:26.40	Loktin and Popova (2017)
	06:07:25.68	Kharchenko et al. (2013)
	06:07:25.00	Anderson et al. (2013), Wu et al. (2009) Dias et al. (2002)
DEC (deg)	24.109±0.070	Present study
DEC (dd:mm:ss)	24:06:32.40	Present study
	24:05:56.40	Cantat-Gaudin et al. (2018)
	24:05:52.80	Loktin and Popova (2017)
	24:05:31.20	Kharchenko et al. (2013)
	24:05:48.00	Anderson et al. (2013), Wu et al. (2009) Dias et al. (2002)
ℓ (deg)	186.629	Present study
	186.635	Cantat-Gaudin et al. (2018)
	186.704	Loktin and Popova (2017)
	186.635	Kharchenko et al. (2013)
	186.634	Anderson et al. (2013), Wu et al. (2009) Dias et al. (2002)
b (deg)	1.796	Present study
	1.788	Cantat-Gaudin et al. (2018)
	1.786	Loktin and Popova (2017)
	1.774	Kharchenko et al. (2013)
	1.781	Anderson et al. (2013), Wu et al. (2009) Dias et al. (2002)

within each ring and their number divided by the area of each ring. A King (1966) model is then fitted to the radial density profile of NGC 2158 as shown in Figure 6.

$$\rho(R) \;=\; f_{bg} + \left[\frac{f_0}{1 + (R/R_{core})^2}\right], \qquad (1)$$

where f_{bg}, f_0 and R_{core} are the background density, the central star density and the core radius of the cluster, respectively. The best-fit values are $f_0 = 67.06 \pm 2.47$ stars/arcmin^2 and $R_{core} = 1'.70 \pm 0'.08$ see Table 3. The limiting radius of NGC 2158 is estimated as $R_{lim} = 17'.00$, beyond which stars begin to merge with the background population (see Figure 6, Tadross and Hendy

TABLE 3

THE RDP PARAMETERS OF THE OPEN CLUSTER NGC 2158

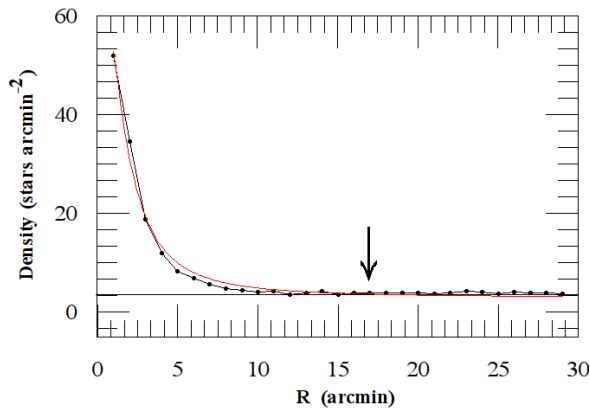| Parameter	Values	Reference
R_{lim} (arcmin)	17.00	Present study
	15.00	Kharchenko et al. (2013)
	18.60	Anderson et al. (2013)
	07.50	Glushkova et al. (2010)
R_{core} (arcmin)	01.70±0.08	Present study
	02.40	Kharchenko et al. (2013)
	01.71	Anderson et al. (2013)
Concentration parameter (C)	01.00	Present study
f_0 (stars/arcmin^2)	67.06±2.47	Present study

Fig. 6. The radial density profile of NGC 2158. The red curved line is our best-fit King profile). The value of the limiting radius is $R_{lim} = 17\!.\!00$. The solid line represents the background density. The color figure can be viewed online.

2016; Hendy 2018). Following Peterson and King (1975), we find that the concentration parameter $C = \log s\,(R_{lim}/R_{cor})$ of NGC 2158 is $C = 1.00$.

Our estimations of the core and limiting radii are in very good agreement with the ones obtained by Anderson et al. (2013) and Kharchenko et al. (2013), see Table 3, but the limiting radius obtained by Glushkova et al. (2010) is significantly smaller than the one we find.

2.3. Color Magnitude Diagrams

To obtain photometric data for multi-color magnitude diagrams (MCMDs), we cross-matched our cluster members in Figure 4 with Gaia, 2MASS and BV data from Nardiello et al. (2015). We obtained 1223 common stars which are members of the cluster. The MCMDs of NGC 2158 are built using optical data from Gaia DR2 $[G, (G_{BP}-G_{RP})]$, Nardiello

et al. (2015) $[V, (B - V)]$ and infrared 2MASS data $[J, (J - H)$ and $J-, J - K)]$ are shown in Figure 7.

To obtain the best fit for each CMD, we use the Padova isochrones of Marigo et al. (2017) with a solar metallicity of 0.0152 (Bressan et al. 2013). Using the turn-off point, we find an age of $\log \text{age} = 9.350 \pm 0.050$, that is, and age of 2.240 ± 0.260 Gyr. The extinction ratios used for correcting the magnitudes come from the following transformation equations, based on the work by Cardelli et al. (1989) and O'Donnell (1994):

$$R_V = \frac{A_V}{E(B-V)} = 3.1, \qquad (2)$$

$$\frac{A_G}{A_V} = 0.861, \qquad (3)$$

$$\frac{A_J}{A_V} = 0.296, \qquad (4)$$

$$\frac{A_K}{A_V} = 0.116, \qquad (5)$$

and hence

$$\frac{E(B-V)}{E(G_{BP}-G_{RP})} = 0.785, \qquad (6)$$

$$\frac{E(B-V)}{E(J-H)} = 2.842, \qquad (7)$$

$$\frac{E(B-V)}{E(J-K)} = 1.792. \qquad (8)$$

Table 4 lists the comparison between the fundamental parameters of NGC 2158 obtained here and those obtained in other studies. Using the inferred values of the photometric color excess of NGC 2158, we found that $E(G_{BP} - G_{RP}) = 0.590$, $E(J - H) = 0.160$ and $E(J - K) = 0.220$. The mean color excess $E(B - V)$ and the intrinsic distance modulus $(m - M)_0$ are 0.420 ± 0.050 mag and
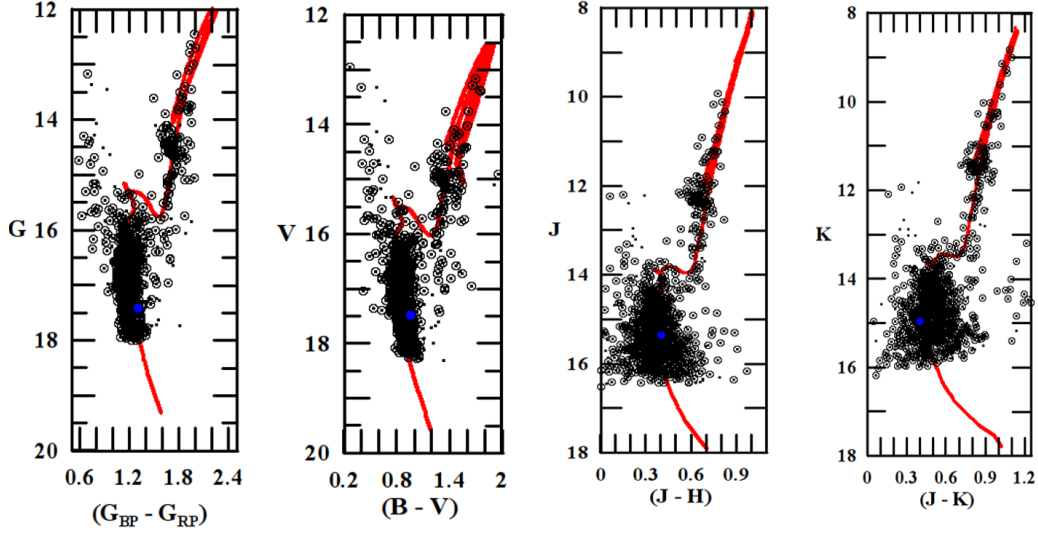
Fig. 7. CMDs of NGC 2158: $[G - (G_{BP} - G_{RP})]$ from Gaia DR2, $[V - (B - V)]$ from Nardiello et al. (2015) and $[J - (J - H) \& J - (J - K)]$ from 2MASS data respectively. The blue circles in the CMDs refer to the position of the eclipsing binary [NBN2015]78. The dots represent 1223 member stars in the optical (Gaia & $[V - (B - V)]$), and the 2MASS data using our criteria. The open circles represent 1031 membesr stars obtained by Cantat-Gaudin et al. (2018) using their UPMASK code to determine membership probabilities. The color figure can be viewed online.

12.540 ± 0.130 mag respectively. $E(B - V)$ and $(m - M)_0$ are in a good agreement with those estimated by Glushkova et al. (2010), Tadross (2001); Loktin et al. (2001); Dias et al. (2002) and Bedin et al. (2010), see Table 4. The distance of NGC 2158 from the Sun is $d_\odot = 3224 \pm 200$ pc, in good agreement with that of Glushkova et al. (2010).

Cantat-Gaudin et al. (2018) calculated the distance of 1229 open clusters by using the UPMASK code of probable cluster members with probabilities larger than 50%. Lindegren et al. (2018) found that the Gaia DR2 parallaxes are affected by a zero-point offset of -0.029 mas. Cantat-Gaudin et al. (2018) reported in their Table 1 (Vizier database reference J/A+A/618/A93) the distance and its uncertainties d, d_+ and d_- as 4535.1, 3119.8 and 8301 pc respectively[4]. We estimate a distance of $d_\odot = 3224 \pm 200$ pc using the best fit of the isochrones in the multi-color magnitude diagrams of optical and 2MASS data (Figure 7), in a good agreement with the smaller value of $d_+ = 3119.8$ pc of Cantat-Gaudin et al. (2018).

The published parallax of the eclipsing binary [NBN2015]78 in Gaia DR2 is $\varpi = 2.202 \pm 0.409$ mas, a relative uncertainty smaller than 20%. We determine the distance of this binary as $d_{EB}(Gaia) =$

454.2 pc using the inverse of the Gaia parallax. This distance to [NBN2015]78 is much smaller than the mean distance to NGC 2158 $d_\odot = 3224 \pm 200$ pc, and therefore [NBN2015]78 is a foreground field star and not a cluster member.

Following Tadross (2011) we assume that the Sun lies at distance 8.2 kpc from the Galactic center, and find, for the following parameters: the distance of NGC 2158 from the Galactic center (R_{gc}), the projected distances on the Galactic plane from the Sun $(X_\odot$ and $Y_\odot)$ and the distance from the Galactic plane $(Z_\odot)$ the values $R_{gc} = 11407 \pm 394$ pc, $X_\odot = -3201 \pm 278$ pc, $Y_\odot = -372 \pm 32$ pc and $Z_\odot = 101 \pm 009$ pc, respectively. These values for R_{gc}, $X_\odot$, $Y_\odot$ and $Z_\odot$ are fully consistent with those of Cantat-Gaudin et al. (2018) using $d_+ = 3119.8$ pc, see Table 4.

3. PHOTOMETRIC STUDY OF THE ECLIPSING BINARY [NBN2015]78

3.1. Data Analysis

The photometric analysis of [NBN2015]78 was carried out using the data obtained by Nardiello et al. (2015), using the SBIG STL-11000M camera attached to the Asiago 67/92 cm Schmidt Telescope, available at the Astronomical Observatory of Padova (OAPD-Osservatorio Astronomico di Padova). The

---

[4]d_+ and d_- are the most likely distances when 0.1 mas is added or subtracted to the maximum likelihood parallax.

TABLE 4

FUNDAMENTAL PARAMETERS OF NGC 2158

| Parameter	Values	References
Solar metallicity	0.0152	Present study
Members (stars)	1223	Present study
	1380	Cantat-Gaudin et al. (2018)
	216	Dias et al. (2002)
log age (yr)	9.350 ± 0.050	Present study
	9.330	Kharchenko et al. (2013)
	9.300 ± 0.100	Glushkova et al. (2010)
	9.301	Chen et al. (2003) & Bedin et al. (2010)
	9.200	Tadross (2001)
$E(B - V)$	0.420 ± 0.050	Present study
	0.368 ± 0.021	Loktin & Popova (2017)
	0.333	Kharchenko et al. (2013)
	0.340 ± 0.030	Glushkova et al. (2010)
	0.420	Bedin et al. (2010)
	0.360	Loktin et al. (2001) & Dias et al. (2002)
	0.400	Tadross (2001)
$E(G_{BP} - G_{RP})$	0.590	Present study
$E(J - H)$	0.160	Present study
	0.107	Kharchenko et al. (2013)
$E(J - K)$	0.220	Present study
	0.160	Kharchenko et al. (2013)
$(m - M)_{\odot}$	12.540 ± 0.130	Present study
	13.545 ± 0.082	Loktin & Popova (2017)
	12.580 ± 0.200	Glushkova et al. (2010)
	12.980	Bedin et al. (2010)
$d_{\odot}$ (pc)	3224 ± 200	Present study
	3119.800	Cantat-Gaudin et al. (2018)
	4770	Kharchenko et al. (2013)
	3300 ± 300	Glushkova et al. (2010)
	5071	Dias et al. (2002), Wu et al. (2009) & Gozha et al. (2012)
	3600	Carraro et al. (2002) & Chen et al. (2003)
	5012	Tadross (2001)
R_{gc} (pc)	11407 ± 394	Present study
	11444	Cantat-Gaudin et al. (2018)
	13050	Gozha et al. (2012)
$X_{\odot}$ (pc)	-3201 ± 278	Present study
	-3097	Cantat-Gaudin et al. (2018)
	-13035	Wu et al. (2009)
	-5035	Gozha et al. (2012)
$Y_{\odot}$ (pc)	-372 ± 032	Present study
	-360	Cantat-Gaudin et al. (2018)
	-586	Wu et al. (2009) & Gozha et al. (2012)
$Z_{\odot}$ (pc)	101 ± 009	Present study
	97.300	Cantat-Gaudin et al. (2018)
	158	Wu et al. (2009) & Gozha et al. (2012)
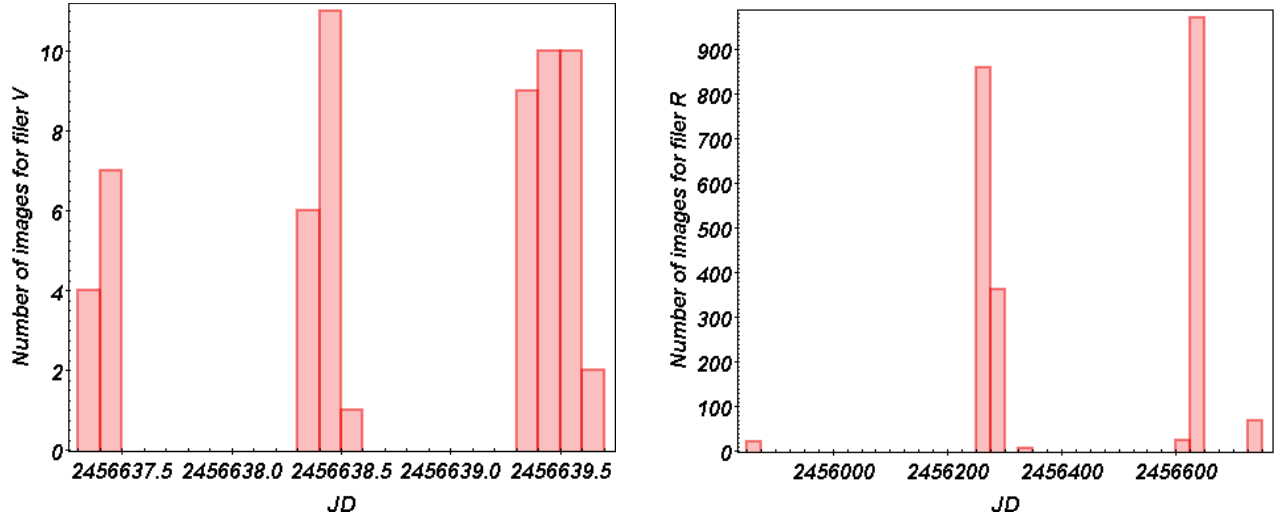
Fig. 8. Histogram of the number of images collected per night during the three campaigns. The histograms refer to observations in the V and R filters. The color figure can be viewed online.

TABLE 5

LOG OF OBSERVATIONS

Filter	# Images	Exp. time (s)	FWHM (arcsec)	Median FWHM (arcsec)
V	60	180	1.24-2.05	1.43
R	1385	15	1.35-6.34	2.75
	27	120		
	2552	180		

V, R data were collected from a number of images gathered over the three seasons. Table 5 presents the total number of observations in each filter as obtained from Nardiello et al. (2015) and Figure 8 shows the histogram of the observations in each filter.

The period and the times of primary (I) and secondary (II) minima of [NBN2015]78 were obtained for the V and R filters (see Table 6). Using the method of Kwee and Woerden (1956), we infer that the new ephemeris for the system is given by

$$\mathrm{HJD}(MinI) = 2456639.55464 \pm 0.0015 + 0.341325^{d} \times E, \quad (9)$$

where E is the integer number of cycles. This ephemeris is used to calculate the phases and to draw the light curves in the V and R bands as shown in Figure 9.

3.2. Light Curve Analysis

The light curve analysis of the system [NBN2015]78 is performed using the light curves in both V and
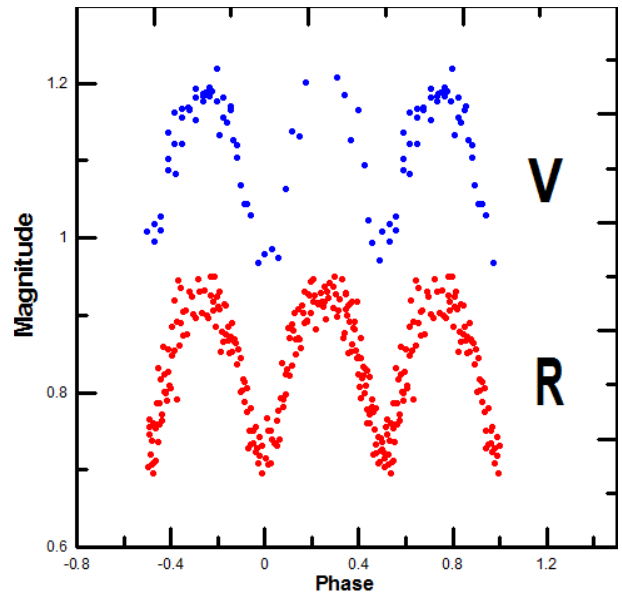

Fig. 9. The observed phase diagram of [NBN2015]78 in the V and R filters. The color figure can be viewed online.

R bands and is carried out using the program of Wilson-Devinney (W-D, Nelson 2009; Wilson and Devinney 1971). We assumed gravity darkening and bolometric albedo exponents appropriate for the convective envelopes of late-type stars ($T_{\mathrm{eff}} < 7500\,K$). We adopted $g_1 = g_2 = 0.32$ (Lucy 1967) and $A_1 = A_2 = 0.5$ (Rucinski 1969). The limb-darkening coefficients were interpolated from the tables of van

TABLE 6

TIMES OF PRIMARY AND SECONDARY
MINIMA OF [NBN2015]78

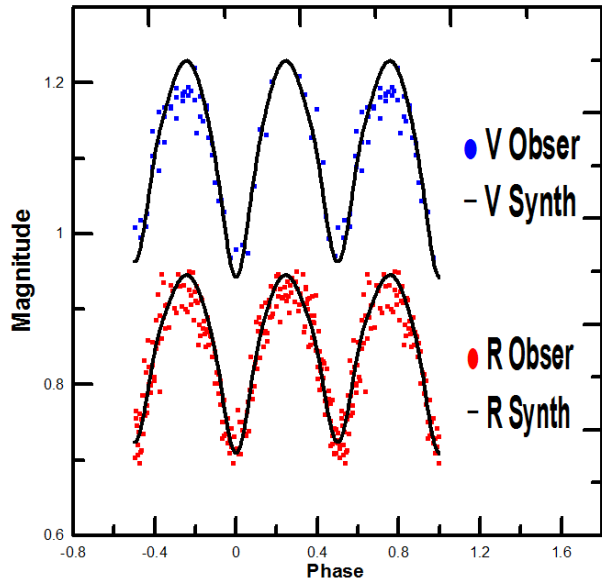| Filter	MinI	MinII
V	2456639.555 ± 0.002	2456638.351 ± 0.0001
R	2456639.547 ± 0.002	2456639.384 ± 0.0002

Fig. 10. V, R filters for the system [NBN2015]78 as fitted with the synthetic model (sold line). The color figure can be viewed online.

TABLE 7

THE ORBITAL SOLUTION FOR [NBN2015]78 IN
V AND R BANDS

Parameter	V	R
λ (Å)	5500	7000
T_1 (K)	4925	4925
T_2 (K)	4780 ± 107	4760 ± 062
q	0.263 ± 0.035	0.262 ± 0.010
$\Omega_1 = \Omega_2$	2.354 ± 0.075	2.374 ± 0.023
$g_1 = g_2$	0.320	0.320
$A_1 = A_2$	0.500	0.500
$X_1 = X_2$	0.643 ± 0.076	0.643 ± 0.028
$Y_1 = Y_2$	0.160	0.160
i (°)	69.530 ± 2.900	67.500 ± 1
r pole1	0.468	0.473
r side1	0.505	0.512
r back1	0.530	0.538
r pole2	0.253	0.259
r side2	0.264	0.270
r back2	0.297	0.308
$\frac{L_1}{L_1+L_2}$	0.797 ± 0.050	0.799 ± 0.020
$\sum(o-c)^2$	0.020	0.160

TABLE 8

ABSOLUTE PHYSICAL PARAMETERS FOR
[NBN2015]78

Element	$M(M_\odot)$	$R(R_\odot)$	$T(T_\odot)$	$L(L_\odot)$	M_{bol}	$Sp.type$
Primary	0.817	0.912	0.852	0.439	5.588	K1
Secondary	0.214	0.858	0.827	0.345	5.849	K2

Hamme (1993) using the logarithmic law and the values $X1 = X2$ and $Y1 = Y2$ for the over-contact mode. The effective temperature of the primary star (T_1) is adopted as 4925 K (Flower 1996), corresponding to a $B-V$ color index of 0.959 from the combined light of both components (Nardiello et al. 2015). The adjusted parameters are the orbital inclination (i), the mean temperature of the secondary star (T_2), the potential of the two components $\Omega = \Omega_1 = \Omega_2$, the mass ratio ($q$), and the luminosity of the primary star (L_1). We used Mode 3 in the Wilson-Devinney (W-D) program (over-contact mode not in thermal contact). The orbital solutions using both V and R light curves are performed and the accepted parameters are listed in Table 7. Figure 10 shows the best match between the model and the observed light curves. The solution shows that the primary component is the more massive and the hotter one, with a difference in effective temperature equal to 145 K. According to this solution, the two components of [NBN2015]78 are of spectral types K1 and K2 (Covey 2007).

Figure 11 shows the geometric configuration of [NBN2015]78 at different phases and the corresponding Roche lobe geometry. The absolute physical parameters of the system are calculated using the empirical relations of Harmanec (1988). The mass of the primary component $M_1 = 0.817 M_\odot$, while the mass of the secondary component is directly calculated from the estimated mass ratio of the system ($q = M_2/M_1$) as $M_2 = 0.214 M_\odot$. The radii of the two components $R_1(R_\odot)$; $R_2(R_\odot)$ and the bolometric magnitudes M_{1bol} and M_{2bol} also calculated and listed in Table 8.

3.3. Evolutionary Status of [NBN2015]78

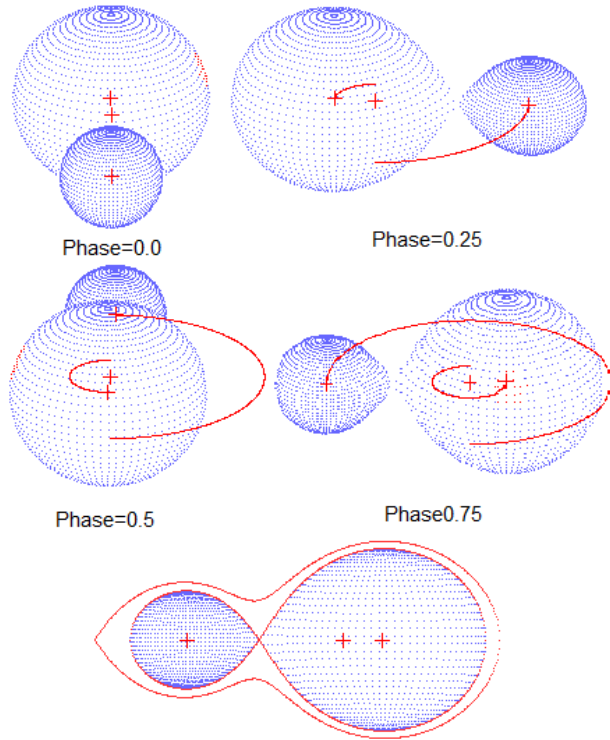Using the calculated physical parameters listed in Table 8 we investigated the current evolutionary sta-

Fig. 11. Geometric configuration at different phases of [NBN2015]78. The color figure can be viewed online.

tus of the system. Figure 12 shows the components of the system in the mass-luminosity (M-L, left panel), mass-radius (M-R, middle panel) and mass-temperature (M-T, right panel) relations, along with evolutionary tracks computed by Mowlavi et al. (2012) for both zero age main sequence (ZAMS) and terminal age main sequence (TAMS) with solar metallicity ($Z_\odot = 0.014$).

The right panel also shows the location of the components on the empirical $M - T_{\rm eff}$ relation for intermediate mass stars from Malkov (2007). As it is clear from Figure 12 (left and middle panels) the primary component is lying on the ZAMS track while the secondary component is an evolved star.

4. DISCUSSION AND CONCLUSIONS

Using a combination of all the available photometric and astrometric data from the Gaia DR2 and 2MASS catalogues, we presented the optical, near-IR photometric and astrometric properties of the intermediate-age open cluster NGC 2158 and an eclipsing binary system [NBN2015]78 which is found within the same field. The main results of this study can be summarized as follows:

- The cluster membership investigation was performed using a criterion based on the high-

precision Gaia proper motions. We found 1223 member stars in Gaia, 2MASS and the BV catalogue of Nardiello et al. (2015), 1031of which being in the catalog of Cantat-Gaudin et al. (2018) with high membership probabilities, above $> 60\%$.

- Using multi-color magnitude diagrams (Gaia DR2, optical BV, 2MASS), we determined the age, colour excess and distance of NGC 2158 as $2.240 \pm 0.260\,{\rm Gyr}$, $0.420 \pm 0.050\,{\rm mag}$ and $3224 \pm 200\,{\rm pc}$, respectively.

- Using the high-precision Gaia proper motions, we found that the position of the eclipsing binary [NBN2015]78 in VPD is very far away from the cluster region. It is clearly seen that the direction of the proper motion vector of [NBN2015]78 is different from the direction of the cluster members.

- We analyzed the light curves in the V and R bands of the system [NBN2015]78 using the W-D code to obtain the geometric and photometric parameters of the system.

- The [NBN2015]78 system is an over-contact binary with a fill-out factor=17.5% and a low mass ratio $q = 0.262$.

- The system is classified as being of the A-subtype and the components have spectral types K1 and K2.

- The positions of both components of [NBN2015]78 in the mass-radius and mass-luminosity relations reveal that the primary component is a main sequence star while the secondary is an evolved component.

- The distance to [NBN2015]78 is 454.2 pc, while the mean distance to the NGC2158 is equal to 3224 ± 200 pc, so we can confirm that the binary system [NBN2015]78 is definitely one of the foreground field stars.

A series of new photometric and spectroscopic observations of [NBN2015]78 is highly recommended for a detailed study of its period stability and to determine more precise physical parameters.
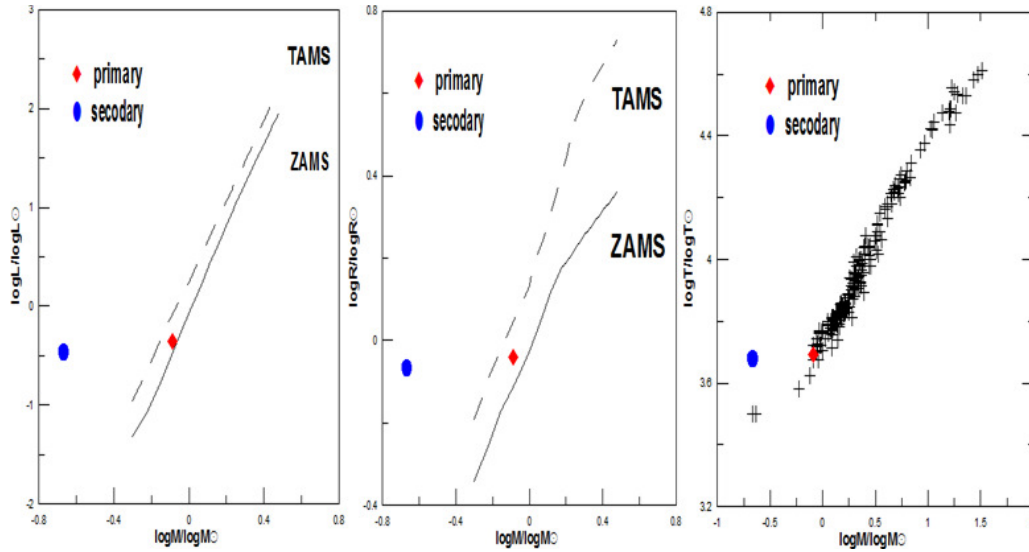
Fig. 12. The position for the components of the system on the mass-luminosity (left), mass-radius (middle) and empirical $M - T_{\rm eff}$ relation (right) for intermediate mass stars. The color figure can be viewed online.

REFERENCES

Anderson, R. I., Eyer, L., & Mowlavi, N. 2013, MNRAS, 434, 2238

Bedin, L. R., Salaris, M., King, I. R., et al. 2010, ApJ, 708, 32

Bisht, D., Yadav, R. K. S., & Ganesh, S. 2019, MNRAS, 482, 1471

Bonnarel, F., Fernique, P., Bienaymé, O., et al. 2000, A&AS, 143, 33

Bressan, A., Marigo, P., Girardi, L., Nanni, A., & Rubele, S. 2013, EPJWC, 43, 03001

Cantat-Gaudin, T., Jordi, C., Vallenari, A., et al. 2018, A&A, 618, 93

Cardelli, J. A., Clayton, G. C., & Mathis, J. S. 1989, ApJ, 345, 245

Carraro, G., Girardi, L., & Marigo, P. 2002, MNRAS, 332, 705C

Chen, L., Hou, J. L., & Wang, J. J. 2003, AJ, 125, 1397C

Covey, K. R., Ivezić, Ž., Schlegel, D., et al. 2007, AJ, 134, 2398

Dias, W. S., Alessi, B. S., Moitinho, A., & Lepine, J. R. D. 2002, A&A, 389, 871

Ferreira, Filipe A., Santos, J. F. C., Corradi, W. J. B., et al. 2019, MNRAS, 483, 5508F

Flower, P. J. 1996, ApJ, 469, 355

Gaia Collaboration, Prusti, T., de Bruijne, J. H. J., et al. 2016, A&A, 595, A1

Gaia Collaboration, Brown, A. G. A., Vallenari, A., et al. 2018, A&A, 616, A1

Glushkova, E. V., Koposov, S. E., Zolotukhin, I. Yu, et al. 2010, AstL, 36, 75

Gozha, M. L., Borkova, T. V., & Marsakov, V. A. 2012, AstL, 38, 506

Harmanec, P. 1988, BAICz, 39, 329

Hendy, Y. H. M. 2018, JAsGe, 7, 180H

Kharchenko, N. V., Piskunov, A. E., Schilbach, E., et al. 2013, A&A, 558, 53

King, I. R. 1966, AJ, 71, 64

Kwee, K. & Van Worden, H. 1956, BAN, 12, 327

Lindegren, L., Hernandez, J., Bombrun, A., et al. 2018, A&A, 616, A2

Loktin, A. V., Gerasimenko, T. P., & Malysheva, L. K. 2001, A&AT, 20, 607

Loktin, A. V. & Popova, M. E. 2017, AstBu, 72, 257

Lucy, L. 1967, ZA, 65, 89

Lynga, G. 1987, The Open Star Clusters Catalogue, 5th edition: (http://cdsarc.u-strasbg.fr/viz-bin/VizieR?-meta.foot&-source=VII/92A)

Malkov, O. Yu. 2007, MNRAS, 382, 1073

Marigo, P., Girardi, L., Bressan, A., et al. 2017, ApJ, 835, 77

Mowlavi, N., Eggenberger, P., Meynet, G., et al. 2012, A&A, 541, 41

Nardiello, D., Bedin, L. R., Nascimbeni, V., et al. 2015, MNRAS, 447, 3536

Nelson, R. H. 2009, WDwint56a, available from: (https://www.variablestarssouth.org/bob-nelson)

O'Donnell, J. E. 1994, ApJ, 422, 158

Peterson, C. J. & King, I. R. 1975, AJ, 80, 427

Ruciński, S. M. 1969, AcA, 19, 125

Saad, M. S., Darwish, M. S., Nasser, M. A., et al. 2016, NewA, 47, 24S

Skrutskie, M. F., Cutri, R. M., Stiening, R., et al. 2006, AJ, 131, 1163

Stassun, K. G. & Torres G. 2018, ApJ, 862, 61S

Tadross, A. L. 2001, NewA, 6, 293

_____. 2011, JKAS, 44, 1

Tadross, A. L. & Hendy, Y. H. M. 2016, JKAS, 49, 53T

Taylor, M. B. 2005, ASPC, 347, 29

Van Hamme, W. 1993, AJ, 106, 2096

Wilson, R. E. & Devinney, E. J. 1971, ApJ, 166, 605

Wu, Z-Y., Zhou, X., Ma, J., & Du, C-H. 2009, MNRAS, 399, 2146

A. E. Abdelaziz, Y. H. M. Hendy, S. M. Saad, and A. Shokry: Astronomy Department, National Research Institute of Astronomy and Geophysics (NRIAG), Helwan, Cairo, Egypt (abdelazizeid3, y.h.m.hendy@gmail.com).

K. A. Edris and F. Y. Kamal: Department of Astronomy and Meteorology, Faculty of Science, Al-Azhar University, Cairo, Egypt.

S. M. Saad: Kottamia Center of Scientificc Excellence for Astronomy and Space Sciences (KCScE), STDF No. 5217.